

PARTICULAR ASPECTS REGARDING MAGNETIZATION REVERSAL IN NANODIMENSIONAL MAGNETIC NANOSTRUCTURES FOR SPINTRONICS AND SENSORISTICS

Andrei KUNCSE¹, Stefan ANTOHE^{2,3}

Abstract. *Understanding the nanoscale magnetic behavior in low-dimensional systems is essential for the development of novel recording systems and miniaturized high performance sensors. In this paper, special features of magnetic domains/ magnetic domain walls propagation are approached for 1D cylindrical nanowires and rectangular stripes form Ni-based permalloy. A method for domain wall injection and velocity manipulation by electric current has been indicated based on theoretical results from micromagnetic simulations performed using Object Oriented Micromagnetic Framework (OOMMF) software.*

Keywords: micromagnetic, nanostructures, spintronics, magnetization reversal

1. Introduction

The growing demand of cheap and optimized magnetic sensors on a hand, and magnetic recording media on the other hand, led in the past few years to an extensive research on novel principles of magnetic recordings. One of the proposed directions implies the transition from data manipulation via magnetic fields to data manipulation via electric currents, as well as the transition from the classical noninteracting monodomain-like ‘bits’ to a data storage via domain/domain walls or other magnetic configuration which could be accordingly manipulated. Therefore, the subject of the manipulation of magnetic domains/domain walls by either magnetic fields or electrical currents is under an intensive debate both from a fundamental point of view as well as from a technological point of view, e.g. regarding especially spintronics [1-4] and sensoristics [5, 6] applications. The continuous growth of data storage capacity as well as the permanent increase in the sensitivity of various sensors can be sustained only by a deep understanding of the processes occurring in nanostructured magnetic systems. The new developments in the field of magnetic recording, spintronics and sensoristics (e.g. detecting weak magnetic fields or the possibility of a suitable control and detection of functionalized nanoparticles for biomedical applications) are strictly related to the possibility of designing suitable

¹Researcher, PhD, National Institute of Materials Physics, Magurele, Romania

²Prof., PhD, University of Bucharest, Faculty of Physics, 405 Atomistilor Street, P.O. Box MG1, 077125, Magurele, Romania

³Academy of Romanian Scientists, Splaiul Independentei 54, 0505094, Bucharest, Romania.

mechanisms for a reliable control (movement as well as pinning) of the magnetic domains/domain walls in such nanosized magnetic systems. In this respect, the main interest concerns the pinning or the displacement of the magnetic domains in textured media as well as in low dimensional systems: bidimensional (2D-nanometer thick thin films), unidimensional (1 D-nanowires, nanoroads, nanotubes) and 0 dimensional (0D-nanoparticles).

As an example, regarding unidimensional magnetic nanosystems, nanowires with well controlled sizes and shapes are extensively studied in the last few years from the point of view of their special magnetic and magneto-conduction properties, anticipating their huge potential in technological applications ranging from magnetic recording [7] [8] to spintronics [9]. The so-called racetrack memories [7] [10] rely on a proper association of the binary states to specific domain walls injected in nanowires matrices; data handling is based on the manipulation and detection of the domain walls as they pass through reading/writing heads. A great increase in the speed of data manipulation and also an increase in the storage capacity it is aimed with this type of memory. On the other hand, concerning 1D systems there is also a huge interest from the fundamental point of view, the magnetic nanowires being perfect subjects for the study of very particular magnetic aspects in relation to geometrical and morphological aspects.

Regarding the 0D systems, functionalized magnetic nanoparticles can be used in biomedical applications [11-13] for both diagnoses (magnetic resonance imaging) and treatments (systems of nanoparticles under radiofrequency magnetic fields induce local hyperthermia and can be used for cancer treatment or controlled drugs release). Both the formation and displacement (electrically or magnetically induced) of magnetic domains as well as their reconfiguration under various excitations involve very complex phenomena which depend on the intrinsic magnetic properties of the material as well as on the geometrical, morphological and structural aspects, including the presence of defects. The optimization of the formation and displacement of magnetic domains with respect to a particular application requires a suitable design and production of the system followed by an extensive morphological, structural and magnetic experimental characterization. Concerning the first step, micromagnetic simulations performed with programs which employ finite difference methods are extensively used for the design of magnetic systems with particular properties and for the prediction of their magnetic behavior. Without any doubts, the theoretical approach must be in a continuous correlation with suitable experiments and also requires reliable magnetic parameters as input, to be only experimentally derived. Any approach of the phenomena inside low dimensional magnetic structures (nano/microscopic) starts from a proper description of the significant energetic terms characterizing the investigated systems, which will be briefly discussed in the following.

2. Mathematical descriptions

The magnetic configuration in a magnetic system is generally provided by the simultaneous action of 4 types of energies: exchange (E^{sch}), demagnetization (E^{demag}), magneto-crystalline (E^{aniz}) and Zeeman (E^{zeeman}). Estimation and minimization of the total energy described by the sum of the 4 terms above, leads to the prediction of the magnetic configuration in a stationary state. On the other hand, by expressing the total energy in terms of effective field acting on the investigated magnetic moment, the evolution of the magnetic system in time is described by the Landau-Lifshitz-Gilbert equation. Consequently, there is a stationary approach and a time-dependent approach regarding the structure of magnetic moments in the system and both of them require specific definitions of energy terms.

Consider a magnetic system divided in small rectangular cells with volume dV , each cell with an associated magnetic moment $|\mathbf{m}_i| = M_s dV_i$ where M_s is the spontaneous (experimentally approached by the saturation) magnetization of the system. The problem of finding the stable configuration (distribution in space) of magnetic moments restricts at finding that particular set of magnetic moments which minimizes the total energy [14-16] of the magnetic system:

$$E^{\text{tot}} = E^{\text{zeeman}} + E^{\text{sch}} + E^{\text{aniz}} + E^{\text{demag}} \quad (1)$$

In order to solve the minimization problem (based on vanishing derivative of total energy), each of the above terms must be described [14-16] in the frame of a discretized system.

Zeeman energy (total energy density of the magnetic moments under the influence of external magnetic field) is described as the sum of independent energies of magnetic moments under the same external magnetic field.

$$E^{\text{zeeman}} = \sum_i \mathbf{m}_i \mathbf{H}_i^{\text{ext}} \quad (2)$$

Exchange energy is conveniently described considering the short distance nature of the exchange interaction (e.g. when dealing with localized magnetic moments). Thus, each magnetic moment is influenced only by its 6 nearest neighbors (localized in cubic/tetragonal cells). The total exchange energy density is accordingly defined by:

$$E^{\text{sch}} = \sum_i \sum_{j \in N_i} A_{ij} \frac{\mathbf{m}_i \cdot (\mathbf{m}_i - \mathbf{m}_j)}{\Delta_{ij}^2} \quad (3)$$

where N_i represents the 6 nearest neighbors of cell i , A_{ij} is the stiffness constant between cell i and j and Δ_{ij} is the distance between two cells. The stiffness constant is defined within the investigated system. Consequently, if the neighboring cells have the same magnetic parameters then $A_{ij}=A$ where A represents the stiffness constant of the magnetic material inside cell i/j . When the magnetic parameters are different, the approximation $A_{ij}=2A_iA_j/(A_i+A_j)$ can be employed; if this is not satisfactory, A_{ij} can be manually introduced.

If a Ruderman-Kittel-Kasuya-Yosida (RKKY) interaction is employed between the magnetic moments on two different surfaces (non-localized magnetism), then the exchange energy is defined as [17]:

$$E^{sch} = \sum_i \sum_{j \in N_i} \frac{\sigma_1 [1 - \mathbf{m}_i \cdot \mathbf{m}_j] + \sigma_2 [1 - (\mathbf{m}_i \cdot \mathbf{m}_j)]}{\Delta_{ij}^2} \quad (4)$$

where σ_1 and σ_2 are the exchange coefficients between the two surfaces.

Magneto-crystalline anisotropy energy is related to the spin-orbit interactions inside the system and is dependent on its crystal structure. If the anisotropy is uniaxial, then the density of anisotropy energy is defined as:

$$E_i = \sum_i K_i (1 - \mathbf{m}_i \cdot \mathbf{u}_i)^2 \quad (5)$$

where K_i is the positive magneto-crystalline anisotropy constant, \mathbf{m}_i the magnetic moment associated to cell i and \mathbf{u}_i is the unit vector which describes the direction of the anisotropy axis. If θ is the angle between the directions of the magnetic moment and the direction of the unit vector \mathbf{u}_i , the density of crystalline anisotropy is defined as:

$$E_i^{anis} = \sum_i K_i \sin^2 \theta_i \quad (6)$$

In the case of cubic anisotropy, the energy density is defined as:

$$E_i^{anis} = \sum_i K_i (a_1^2 a_2^2 + a_2^2 a_3^2 + a_3^2 a_1^2) \quad (7)$$

where $a_1 = \mu u_1$, $a_2 = \mu u_2$, $a_3 = \mu u_3$, \mathbf{u}_1 , \mathbf{u}_2 and \mathbf{u}_3 describe the anisotropy directions.

The demagnetization energy due to dipolar interactions is the most difficult to evaluate, considering its long-range influence. To evaluate the demagnetizing field (and consequently the energy) on each cell there must be performed an integral over the entire magnetic domain (all the magnetic moments influence each other through dipolar interactions) which for realistic systems is not feasible. Instead,

mean field methods are employed, each magnetic moment being considered to act independently under the action of an effective field which is result to the multiple interactions in the system.

$$H_{i_1 i_2 i_3}^{demag} = - \sum_{j_1=1}^{n_1} \sum_{j_2=1}^{n_2} \sum_{j_3=1}^{n_3} N(r_{i_1 i_2 i_3} - r_{j_1 j_2 j_3}) \mathbf{m}_{j_1 j_2 j_3} \quad (8)$$

In the expression above a 3d system with n_1 , n_2 and n_3 discretization points along x , y respectively z axis is considered. The triple $i_1 i_2 i_3$ index is used to index the position of the cell in space, the $r_{i_1 i_2 i_3}$ vector represents a displacement vector and $\mathbf{m}_{j_1 j_2 j_3}$ describes the magnetization of the corresponding cell; $N(r)$ is a demagnetization tensor associated to the same cell and is computed according to [18-20].

According to the relations above, the total energy can be expressed as:

$$E^{tot} = \sum_i (\mathbf{m}_i \mathbf{H}_i^{ext} + \sum_{j \in N_i} A_{ij} \frac{\mathbf{m}_i \cdot (\mathbf{m}_i - \mathbf{m}_j)}{\Delta_{ij}^2} + K_i (1 - \mathbf{m}_i \cdot \mathbf{u}_i)^2 - \mathbf{m}_i \sum_{j_1=1}^{n_1} \sum_{j_2=1}^{n_2} \sum_{j_3=1}^{n_3} N(r_{i_1 i_2 i_3} - r_{j_1 j_2 j_3}) \mathbf{M}_{j_1 j_2 j_3}) = \sum_i \mathbf{m}_i \mathbf{H}_i^{effect} \quad (9)$$

2.1. Time independent micromagnetic approach

The above expression must be minimized with respect to the system of magnetic moments ($\mathbf{m}_1, \mathbf{m}_2 \dots \mathbf{m}_i \dots \mathbf{m}_N$), which can be described as a $3N$ variables system ($m_{1x}, m_{1y}, m_{1z}, m_{2x}, m_{2y}, m_{2z}, \dots$).

Considering a numerical algorithm based on conjugate gradient method, the evolution towards local energy minima is a consequence of a line minimization sequence. A line is a one-dimensional subspace from the $3N$ dimensional space of all variables (N is the total number of magnetic moments). Once the minimum along a line is found, a new minimization direction is chosen, ideally perpendicular to all other directions.

For a mathematical description of the conjugate gradient method-based algorithms (Fig. 1), the function $\mathbf{y} = \mathbf{y}(x_1, \dots, x_n)$ as well as the corresponding gradient expression $\nabla \mathbf{y} = \frac{\partial \mathbf{y}}{\partial x_1} \mathbf{i}_1 + \frac{\partial \mathbf{y}}{\partial x_2} \mathbf{i}_2 + \dots + \frac{\partial \mathbf{y}}{\partial x_n} \mathbf{i}_n$ with $(\mathbf{i}_1, \mathbf{i}_2, \dots)$ unit vectors is considered.

Let $X^0 = (x_1^0 \dots x_n^0)$ trial solution of the function y and $X^i = (x_1^i \dots x_n^i)$ the refined solution after i iterations of the algorithm. The aim is to find the minima/maxima $y^{\min/\max} = y^{\min/\max}(X^{\min/\max})$ starting from X^0 as initial value.

From vectorial calculus results [21]:

$$\frac{\Delta x_1}{\frac{\partial y}{\partial x_1}} = \frac{\Delta x_2}{\frac{\partial y}{\partial x_2}} = \dots = \frac{\Delta x_n}{\frac{\partial y}{\partial x_n}} = \alpha \quad (10)$$

In the particular case of $\alpha = 1$ (Cauchy's Method) the expression above shows that the „movement” (Δx_i variations) towards the solution is performed exactly along the direction of the gradient.

X^i is iteratively modified towards the minimization/maximization of y using the relation just above. For simplicity we consider $\alpha = 1$ (Cauchy's method). Then:

$$\begin{aligned} x_1^{i+1} &= x_1^i + \Delta x_1 \\ x_2^{i+1} &= x_2^i + \Delta x_2 \\ &\dots \\ x_n^{i+1} &= x_n^i + \Delta x_n \end{aligned} \quad (11)$$

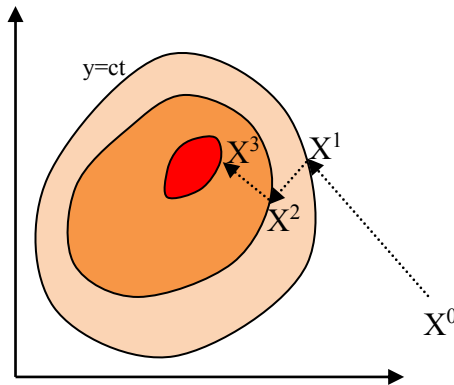


Fig.1. Schematics of Cauchy method for minimizing/maximizing a function

The Cauchy method (particular case for $\alpha = 1$ of Conjugate gradient method) is fast when X^i is far from the acceptable solution $X^{\min/\max}$ but becomes sluggish when the current iteration approaches the solution (directly related to the increasing density of equipotential curves in the $3N$ -dimensional function space). This issue is solved by using subsequently values of α greater than 1

2.2. Time dependent micromagnetic approach

The time evolution of a magnetic moment under the influence of a magnetic field (of any origin) is given by the Landau-Lifshitz-Gilbert [22] equation:

$$\frac{d\mathbf{m}}{dt} = \gamma \mathbf{m} \times \mathbf{H} \quad (12)$$

Where γ is the so-called gyromagnetic factor, m the magnetic moment.

Considering mean field-type approximations, the equation above can be successfully used to predict the evolution of the magnetic system in time. Consequently, the \mathbf{H} field can be defined as a superposition of demagnetizing field, anisotropy-related fields, external fields and a dissipation term.

$$\mathbf{H}^{\text{eff}} = \mathbf{H}_{\text{ext}} + \mathbf{H}_{\text{anis}} + \underbrace{\left(\sum_{\text{vecini ord I}} \mathbf{H}_{\text{sch}} \right)}_{\mathbf{H}_{\text{effect}}} + \mathbf{H}_{\text{demag}} + \frac{\alpha d\boldsymbol{\mu}}{\gamma dt} \quad (13)$$

where $\boldsymbol{\mu} = \frac{\mathbf{m}}{|\mathbf{m}|}$, and α represents an no dimensional parameter (viscosity factor).

Evaluation of the effective field components is straightforward from the total energy term, provided the relation $E = -\mathbf{m} \cdot \mathbf{B}$.

Finally, for a dynamic approach of the magnetic structure, the following equation can be successfully used:

$$\frac{d\mathbf{m}}{dt} = \gamma \boldsymbol{\mu} \times \mathbf{H}_{\text{effect}} + \alpha \boldsymbol{\mu} \times \frac{d\boldsymbol{\mu}}{dt} \quad (14)$$

Equation (14) is to be solved for each magnetic moment (because under the assumption on mean-field approximation each magnetic moment behaves independently) using basic numerical methods such as Cauchy or Runge-Kutta.

3. Simulations in Ni based 1-D nanowires

Lately, nanowires with well-defined shapes and compositions have been extensively investigated with respect to their conduction properties (in the case of semiconductor systems) and regarding their magnetic and magneto-conduction properties (in the case of magnetic systems). The last case is very important relative to both potential technological applications (e.g. magnetic recordings [23] [8], spintronics [9] [17]) and fundamental physics via specific nanometric-scale magnetic effects. Magnetic nanowires represent an excellent support for fundamental studies of the properties and peculiarities of the magnetic structure in one-dimensional nanometric systems with various geometrical and magnetic parameters, as well as under various external excitations (e.g. applied magnetic fields and/or electric currents).

Regarding the technological aspects, initially there have been developed areas (matrices) of ferromagnetic nanowires grown by various methods including the well-known template-method. Within this method, the pores of a specific membrane (e.g. porous alumina [9] [17] or membranes obtained by high energy ion bombardment [24] [25]) are filled with the proper material by electrochemical methods. With this technique, both properties of individual wires (material, shape and geometrical parameters) and collective properties (density of nanowires,

orientation with respect to the template surface) can be controlled. It's worth mentioning that the magnetic properties (including the magnetization reversal) of such complex systems does not depend only on the characteristics of individual wires but also on the interactions between them [26] [27]. Anyway, many applications (spintronics, data storage systems) require non-interacting nanowires, that's why the study of magnetic reversal on individual nanowires remains an important aspect for both fundamental and technological point of view.

Despite its simplicity, the magnetic reversal mechanisms in individual nanowires is very complex (dependent on the material, geometric and experimental configurations and on the excitation type) thus extensively studied in the last decades. Magnetic instabilities which lead to various modes of switching (ex. curling or coherent rotation) have been numerically predicted in the case of long cylindrical nanowires [28]. As intuitively expected, a coherent rotation of the magnetic moments is allowed only for nanowires with diameters smaller than a threshold value, d_{th} close to the dimension of the domain wall, characterized by the so-called exchange-length parameter:

$$\lambda_{ex} = \pi \sqrt{\frac{A}{K}} \quad (15)$$

where A is the stiffness constant and K anisotropy constant. If the shape anisotropy prevails, then K is defined as

$$K = \frac{\mu_0 M_s^2}{4} \quad (16)$$

A critical value $d_t \cong 2 \sqrt{\frac{4\pi A}{\mu_0 M_s^2}}$ has been reported as the threshold for a coherent spin rotation as induced by a magnetic field applied along nanowires axis [29] (according to the relation above, this value is close to domain wall length). More recent simulations performed on soft-magnetic cylindrical nanowires with various diameters or even on conical nanowires have shown that over this threshold value the magnetization takes place in two different ways [30-33]: (i) either in the transverse wall-mode (exchange energy forces an uniform magnetization in each plane perpendicular to the cylinder axis.) or (ii) in vortex-wall mode. The transition between two above mentioned modes is described by a critical value d_c . For both modes the magnetization is changing the sign starting from the nucleation of domain walls on both ends of the nanowire followed by propagation to its center, along the axis. The vortex wall mode contains in each transversal section a point-like singularity (Bloch point) localized on the cylinder axis. Considering the complex magnetic structure of vortex wall mode, is better to

avoid it in a first instance. Practically, this can be done by considering nanowires with diameters d which fulfill the condition $d_{th} < d < d_c$ [32-34].

Identification of d_c parameter is not a trivial problem and micromagnetic simulations performed especially in the case of the soft-magnetic Ni systems reported a d_c value around 40 nm.

Fig. 2. shows the propagation in time of a vortex wall mode and a transverse wall mode as provided by micromagnetic simulations using OOMMF software on a Ni₂₀Fe₈₀ permalloy nanowires with 20 nm and 80 nm diameter, respectively, and an aspect ratio greater than 1:10 [35].

The propagation was analysed in the time dependent configuration with the field applied along the cylinder axis. An exchange stiffness constant $A=13e(-12)$ J/m and a spontaneous magnetization $M_s=8.6e5$ A/m were chosen, as specific to the permalloy material. The spin structure through a section of the nanowire is presented at different moments in Fig.2.

It is observed that in the nanowire with the diameter of 20 nm, all spins in the section rotates gradually at once, whereas in case of the nanowire with 80 nm diameter, inside the same section, the magnetic moments in the center rotate slower than in the outer shells, giving rise to a vortex-like magnetic structure.

In addition, the complete reversal of the magnetic moments through the analyzed section is much faster in case of the vortex-like configuration which is equivalent to an approximately three times higher velocity of the domain walls in case of this last reversal mechanism.

The velocity of transversal domain walls in Ni-Cu alloy nanowires with diameters of 40 nm was estimated for field applied along the axis at about 140 m/s in [36] being shown to be dependent on the orientation of the applied field versus the cylinder axis. In fact, in almost transversal geometry (with the field applied almost perpendicular to the cylinder axis), it has been proven that no domain walls are developed and the magnetic reversal is performed through a coherent like rotation of the magnetic moments.

This aspect might be of high technological interest, while in a coherent (Stoner-Wohlfarth) like rotation, the specific parameters of the hysteresis loops (e.g. the saturation field) can be directly related to M_s and K [37] as well as to specific parameters in magneto-resistance loops [35].

If this is the case, it becomes of direct interest to know the range of diameters where the nanowires present a coherent like rotation in transversal geometry. In this respect, micromagnetic simulations have been performed in the static regime, on Ni-Cu alloy nanowires with diameters ranging from 40 nm to 100 nm. The corresponding hysteresis loops are shown in Fig. 3.

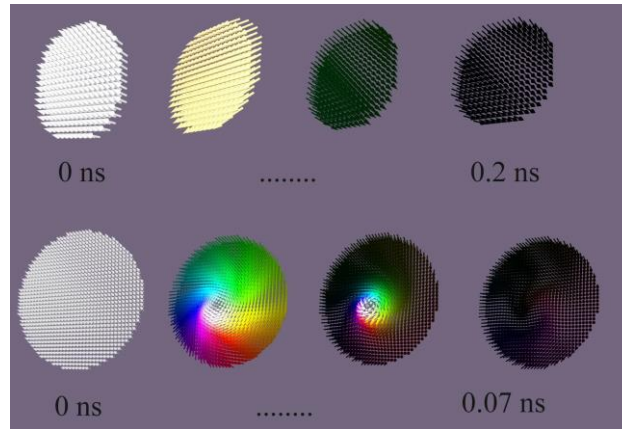


Fig. 2. Micromagnetic simulations on a magnetic permalloy nanowire with two diameters which shows two possible modes of domain wall propagation: transverse wall mode (20 nm diameter nanowire) (up) and vortex wall mode (80 nm diameter) (down); section at the end of the nanowire.

Simulations have been performed starting from reference parameters A and M_s as experimentally obtained in [37] and simulation cell size has been chosen in order to fulfill the maximum spin angle requirements as well as the convergence of the results.

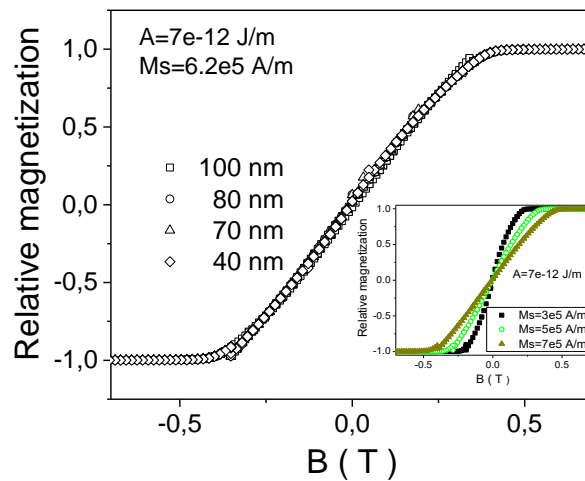


Fig.3. Micromagnetic simulations of static hysteresis loops on Ni-Cu nanowires of different diameters in transversal geometry (with the field perpendicular to the cylinder axis). In inset are presented hysteresis loops obtained on nanowires with a diameter of 100 nm for different values of the spontaneous magnetization.

According to Fig. 3, it may be observed that the hysteresis loops for diameters higher than 40 nm (up to 100 nm in this case) are identical to the one obtained on the nanowire with diameter of 40 nm, supporting an identical (coherent-like) magnetization reversal in perpendicular geometry, independent on the nanowire diameter (to note that transversal or vortex like reversal mechanisms develop for such diameters in longitudinal geometry).

4. Simulations in Permalloy 1-D nanostripes

Simulations of spin/magnetic moment dynamics on one-dimensional structures under applied electric current as performed using OOMMF software extended with the “anv_spinevolve” modulus developed by IMB Zurich Research Center will be also presented in the following.

The presence of electric current density in a magnetic system can be described within micromagnetics by a more general LLG equation, characterized by an additional term which characterizes the spin transfer from free electrons to the localized magnetic moments (an additional torque generated by the misalignment between the spins of injected electrons and the spins which generate the magnetic moments) [38-40]:

$$\frac{d\mathbf{m}}{dt} = \gamma\mathbf{m} \times \mathbf{H}_{\text{effect}} + \alpha\mathbf{m} \times \frac{d\boldsymbol{\mu}}{dt} - (\mathbf{u} \cdot \nabla)\mathbf{m} \quad (17)$$

where \mathbf{u} represents a vector with the direction along the electronic current and with the magnitude $u = \frac{J P \mu_B}{2e M_s}$; J is the current density, P its polarization ($P > 0$ for charge carriers polarized along the orientation of majority of localized magnetic moments) and M_s the spontaneous magnetization, u is measured in velocity units.

Equation above is valid for systems where the domain wall dimension is much lower than the Fermi wavelength/Larmor precession Length/Spin diffusion parameter. Although reasonable from a qualitative point of view, the equation (17) proves major quantitative discrepancies relative to experimental results. These discrepancies cannot be corrected by only considering thermal influences, thus a convenient solution has been found by adding a second order correction to the spin transfer term. The generalized LLG equation becomes:

$$\frac{d\mathbf{m}}{dt} = \gamma\mathbf{m} \times \mathbf{H}_{\text{effect}} + \alpha\mathbf{m} \times \frac{d\boldsymbol{\mu}}{dt} - (\mathbf{u} \cdot \nabla)\mathbf{m} + \beta\mathbf{m} \times [(\mathbf{u} \cdot \nabla)\mathbf{m}] \quad (18)$$

where parameter $\beta \ll 1$, is of same order of magnitude as α . The effect of electric current as it passes through a localized spin system is modeled in OOMMF program using the equation (18).

As exemplification, micromagnetic simulation on a rectangular 500x51x1 permalloy strip initially saturated along Ox axis (the strip is with the long side along Ox axis) are presented [35]. In order to keep simulation restrictions valid (i.e. a proper discretization of the domain walls, maximum angle between magnetic moments bellow 30 degs and convergence of simulations results). A 3x3x1 nm³ discretization cell has been chosen. As parameters characterizing the Ni-Fe type Permalloy, were chosen: stiffness constant $A=13 \times 10^{-12}$ J/m, vanishing magneto crystalline anisotropy and a spontaneous magnetization of 8×10^5 A/m.

The first order dumping parameter α was 0.02 and the second order dumping parameter β was 0.04. The electric current applied along $+Ox$ axis has been swept in the $(3.8 \times 10^{12} \text{ A/m}^2, 4.6 \times 10^{12} \text{ A/m}^2)$ interval and its effect on the structure of magnetic moments has been followed. The effect of a current density of $4.14 \times 10^{12} \text{ A/m}^2$ is shown in Fig. 4. Magnetic moment evolution within 5 ns interval has been followed, showing the time required for a domain wall injection (points a-d in Fig. 4.), the time of propagation of the domain wall along the entire structure (points e-i) and the injection of a second domain wall at the edge of the structure. It is worth mentioning that the misorientation between two successive injected domains walls in 180 degs.

Also, a study of the propagation time with respect to the applied electric current density has been performed and the results are pictured in Fig. 5. In the 2.6×10^{12} - $5.8 \times 10^{12} \text{ A/m}^2$ current density domain, a quasi-linear dependence has been shown.

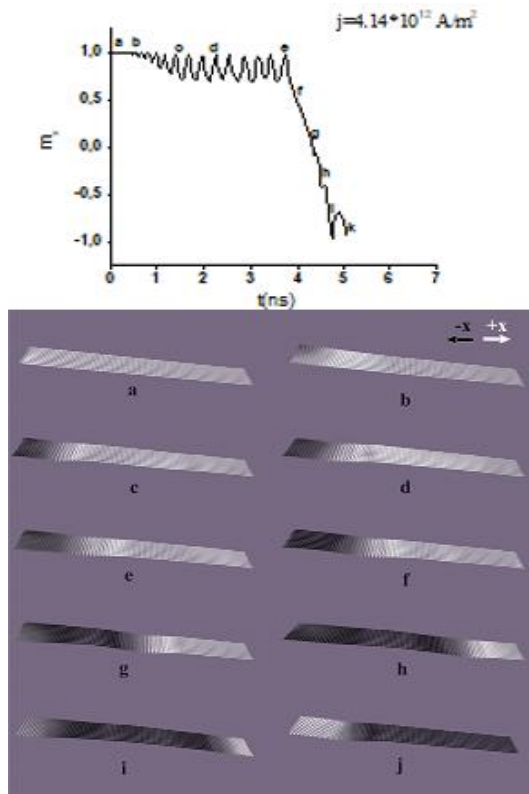


Fig. 4. Injection of domain wall, propagation along the structure, followed by the injection of a second wall.

Fig. 5. Domain wall propagation velocity variation with current density along $+Ox$ axis.

Conclusions

This paper provides an overview of micromagnetic analysis methods employed in the study of nano-dimensional magnetic systems. This is particularly useful for technological applications in spintronics and sensoristics. Understanding how the magnetic structure including domain wall propagation takes place in various low-dimensional magnetic systems under controlled external excitations such as magnetic fields and/or electric currents is still under debate. The best approach for a reliable design of such systems is generally strongly correlated with numerical modeling of the magnetic structure dynamics.

The mathematical instruments used in micromagnetic modeling software based on the minimization of the total energy by numerical methods have been described. The total energy has been expressed by starting from individual contributions of anisotropy, exchange, demagnetization and external fields, based on various approximations (nearest-neighbors interactions, mean field approximations). Magnetization dynamics can be resolved using various expressions of Landau-Lifshitz-Gilbert equation under the assumption that each magnetic moment acts independently but under the influence of an effective field which was evaluated from the total energy expression.

Domain wall propagation in long Ni based nanowires with diameters above the domain wall length has been shown to take place in longitudinal geometry in two different modes (vortex mode and transverse mode) depending on the nanowire diameter, whereas only a coherent type rotation of the magnetic moments is active in transversal geometry.

Also, it has been shown that in the case of magnetic bi-dimensional Permalloy stripes, domain walls can be injected using applied current of the order 10^{12} A/m². The domain wall velocity increases quasi linearly with the current over the considered current density domain.

REFERENCES

- [1] *Spintronics: A Spin-Based Electronics Vision for the Future*. S.A. Wolf, D.D. Awschalom et al. s.l.: Science, **2001**, Vol. 294, pp. 1488-1495.
- [2] *Spintronics: Fundamentals and applications*. I. Žutić, J. Fabian, S. D. Sarma. s.l.: Rev of Modern Phys., **2004**, Vol. 323, pp. 121-139 .
- [3] *Template Nanowires for Spintronics Applications: Nanomagnet Microwave Resonators Functioning in Zero Applied Magnetic Field*. A. Mourachkine, O. V. Yazyev, C. Ducati, J. Ansermet. s.l.: Nano. Lett., **2008**, Vol. 8, pp. 3683-3687.
- [4] *Organic electronics: Spintronics goes plastic*. Sanvito, S. s.l.: Nature. Mat, **2007**, Vol. 6, pp. 803 - 804.

- [5] *Matching domain-wall configuration and spin-orbit torques for efficient domain-wall motion.* A. V. Khvalkovskiy, V. Cros, D. Apalkov, V. Nikitin, M. Krounbi, K. A. Zvezdin, A. Anane, J. Grollier, A. Fert. s.l.: Phys. Rev., **2013**, Vol. 87, p. 020402.
- [6] *Domain wall nanoelectronics.* G. Catalan, J. Seidel, R. Ramesh, J. F. Scott. s.l.: Rev. Mod. Phys., **2012**, Vol. 84, pp. 119-156.
- [7] *Magnetic domain-wall racetrack memory.* S.S. Parkin, M. Hayashi and L. Thomas. s.l.: Science, **2008**, Science, Vol. 320, p. 320.
- [8] *Hexagonally ordered 100 nm period nickel nanowire arrays.* K. Nielsch, R.B. Wehrspohn, J. Barthel, J. Kirschner, U. Gosele, S.F. Fischer, H. Kronmüller. s.l.: Appl. Phys. Lett., **2001**, Vol. 79, pp. 1360-1362.
- [9] *Beating the walker limit with massless domain walls in cylindrical nanowires.* M. Yan, A. Kakay, S. Gliga and R. Hertel. **2010**, Vol. 104, p. 057201.
- [10] *Memory on the racetrack.* S. Parkin, See-Hun Lee. s.l.: Nature Nanotechnology, 2015, Vol. 10, pp. 195-198.
- [11] *Exchange-coupled magnetic nanoparticles for efficient heat induction.* Jae-Hyun Lee, Jung-tak Jang et al. s.l.: Nature Nanotechnology, **2011**, pp. 418-422.
- [12] *Clinical applications of magnetic nanoparticles for hyperthermia.* B. Thiesen, A. Jordan. s.l.: International Journal of Hyperthermia, **2008**, Vol. 24, pp. 467-474.
- [13] *Progress in applications of magnetic nanoparticles in biomedicine.* Q. A. Pankhurst, N.T.K. Thank, S.K. Jones, J. Dobson. s.l.: Journal of Physics D, **2009**, Vol. 42, p. 224001 .
- [14] NIST. *OOMMF user guide.*
- [15] J. Nocedal, S. Wright. *Numerical Optimization.* s.l.: Springer, **2006**.
- [16] *Conjugate gradient method.* Nazareth, J. L. **2009**, Vol. 1, pp. 348–353.
- [17] V. Kuncser, P. Palade et al. Engineering Magnetic properties of nanostructures via Size Effects and Interphase Interactions. *Size Effects in Nanostructures.* Bucharest-Magurele: Springer, **2014**.
- [18] *Demagnetizing factors for rectangular ferromagnetic prisms.* Aharoni, A. s.l.: J. Appl. Phys., **1998**, Vol. 83, pp. 3432-3434.
- [19] *A generalization of the demagnetizing tensor for nonuniform magnetization.* A. J. Newell, W. Williams, D.J. Dunlop. s.l.: Journal of Geophysical Research, **1993**, Vol. 98, pp. 9951-9955.
- [20] *Computing the demagnetizing tensor for finite difference micromagnetic simulations via numerical integration.* D. Chernyshenko, H. Fangohr. s.l.: Computational Physics, **2015**, Vol. 381, pp. 440-445.
- [21] MIT. MIT Open Courseware. <https://ocw.mit.edu/index.htm>. [Online]
- [22] Mansuripur, M. *The physical principles of Magneto Optical Recording.* New York: Cambridge University Press, **1995**.
- [23] *Magnetic domain-wall racetrack memory.* S.S. Parkin, H. Hayashi, L. Thomas. s.l.: Science, **2008**, Vol. 320, pp. 190-194.
- [24] *Magnetic Nanowires.* A. Fert, L. Piraux. s.l.: J. Magn. Magn. Mater., **1999**, Vol. 200, pp. 338-358.

- [25] *Multisegment CdTe nanowire homojunction photodiode*. E. Matei, L. Ion, S. Antohe, I. Enculescu. s.l.: Nanotech, **2010**, Vol. 21, p. 105202.
- [26] *Micromagnetic behavior of electrodeposited cylinder arrays*. C.A. Ross, M. Hwang et al. s.l.: Phys. Rev. B, **2002**, Vol. 65, p. 144417 .
- [27] *Magnetic configurations of Ni–Cu alloy nanowires obtained by the template method*. E. Matei, I. Enculescu, M.E. Toimil-Molaes, A. Leca, C. Ghica, V. Kuncser. s.l.: J. Nanopart. Res., 2013, Vol. 15, p. UNSP 1863.
- [28] *Critical Size and Nucleation Field of Ideal Ferromagnetic Particles*. E.H. Frei, S. Shtrikman, D. Treves. s.l.: Phys. Rev., **1957**, Vol. 106, p. 446 .
- [29] *Magnetization curling in perpendicular iron particle arrays (alumite media)*. G.T.A. Huysmans, J.C. Lodder. s.l.: J. Appl. Phys., **2016**, Vol. 64, pp. 2016-2021 .
- [30] *Micromagnetic simulations of magnetostatically coupled Nickel nanowires*. Hertel, R. s.l.: J. Appl. Phys, **2001**, Vol. 90, pp. 5752-5758.
- [31] *Domain wall motion in nanowires using moving grids*. H. Forster, T. Schrefl, D. Suess, W. Scholz, V. Tsiantos, R. Dittrich, J. Fidler J. s.l.: J.Appl.Phys, 2002, Vol. 91, pp. 6914-6919.
- [32] *Magnetization reversal dynamics in nickel nanowires*. R. Hertel, J. Kirschner. s.l.: Physica B, **2004**, Vol. 343, pp. 206-210.
- [33] *Magnetization Reversal for Ni Nanowires Studied by Micromagnetic Simulations*. N. Han, G. Guo, L. Zhang, G. Zhang, W. Song. s.l.: J. Mater. Sci. Technol, **2009**, Vol. 25, pp. 151-154.
- [34] *A detailed study of magnetization reversal in individual Ni nanowires*. V.E. Vidal, Y.P. Ivanov, H. Mohamed, J. Kosel. s.l.: Appl. Phys. Lett., **2015**, Vol. 106, p. 032403 .
- [35] *Formarea si controlul domeniilor magnetice si/sau a peretilor de domenii pentru diverse aplicatii*, A. Kuncser- PhD thesis held at University of Bucharest, at October **2017**.
- [36] *A general perspective on the magnetization reversal in cylindrical soft magnetic nanowires with dominant shape anisotropy*. A. Kuncser, S. Antohe, V. Kuncser. s.l.: J. Magn. Magn. Mat., **2017**, Vol. 423, pp. 34-38
- [37] *Magnetic configurations of Ni–Cu alloy nanowires obtained by the template method*. E. Matei, I. Enculescu, M.E. Toimil-Molaes, A. Leca, C. Ghica, V. Kuncser. s.l.: J. Nanopart. Res., **2013**, Vol. 15, p. UNSP 1863.
- [38] *Micromagnetic understanding of current-driven domain wall motion in patterned nanowires*. A. Thiaville et al. s.l.: Europhys. Lett., **2005**, pp. 990-996.
- [39] *Roles of nonequilibrium conduction electrons on the magnetization dynamics of ferromagnets*. S. Zhang, Z. Li. s.l.: Phys. Rev. Lett., **2004**, Vol. 93, p. 127204 .
- [40] *Simple model of current-induced spin torque in domain walls*. A. Vanhaverbeke, M. Viret. s.l.: Phys. Rev. Lett., **2007**, Vol. 75, p. 024411 .